Cell Death and Differentiation (2009) 16, 1006–1017
© 2009 Macmillan Publishers Limited All rights reserved 1350-9047/09 $32.00
www.nature.com/cdd

The inositol 1,4,5-trisphosphate receptor regulates autophagy through its interaction with Beclin 1

JM Vicencio[1,2,3,4], C Ortiz[1,2,3,4], A Criollo[1,2,3,4], AWE Jones[5], O Kepp[1,2,3], L Galluzzi[1,2,3], N Joza[1,2], I Vitale[1,2,3], E Morselli[1,2,3], M Tailler[1,2,3], M Castedo[1,2,3], MC Maiuri[1,2,3,6], J Molgó[7], G Szabadkai[5], S Lavandero*[,4,8] and G Kroemer*[,1,2,3,8]

The inositol 1,4,5-trisphosphate receptor (IP_3R) is a major regulator of apoptotic signaling. Through interactions with members of the Bcl-2 family of proteins, it drives calcium (Ca^{2+}) transients from the endoplasmic reticulum (ER) to mitochondria, thereby establishing a functional and physical link between these organelles. Importantly, the IP_3R also regulates autophagy, and in particular, its inhibition/depletion strongly induces macroautophagy. Here, we show that the IP_3R antagonist xestospongin B induces autophagy by disrupting a molecular complex formed by the IP_3R and Beclin 1, an interaction that is increased or inhibited by overexpression or knockdown of Bcl-2, respectively. An effect of Beclin 1 on Ca^{2+} homeostasis was discarded as siRNA-mediated knockdown of Beclin 1 did not affect cytosolic or luminal ER Ca^{2+} levels. Xestospongin B- or starvation-induced autophagy was inhibited by overexpression of the IP_3R ligand-binding domain, which coimmunoprecipitated with Beclin 1. These results identify IP_3R as a new regulator of the Beclin 1 complex that may bridge signals converging on the ER and initial phagophore formation.
Cell Death and Differentiation (2009) **16,** 1006–1017; doi:10.1038/cdd.2009.34; published online 27 March 2009

Macroautophagy (herein referred to as autophagy) is the major catabolic pathway for entire organelles, long-lived/aberrant proteins and superfluous portions of the cytosol. It consists of the stepwise engulfment of substrate elements into distinctive multimembraned autophagosomes, which after fusion with lysosomes form single-membraned autolysosomes. Within the lumen of autolysosomes, macromolecules are enzymatically broken down into metabolites that cope with the bioenergetic and biosynthetic demands of the cell.[1,2]

The molecular activation of autophagy is a complex process (reviewed in Yorimitsu and Klionsky[3]) that is regulated by the mammalian target of rapamycin (mTOR), a protein kinase essential for nutrient-sensing signal transduction.[4] Downstream of mTOR, a series of chain reactions are executed by several autophagy-related (Atg) proteins, allowing the pre-autophagosomal membrane structure (phagophore) to engulf a substrate material, to complete and close the sequestering vacuole in physical association with the microtubular network, and finally fuse autophagosomes with lysosomes to execute degradation. The autophagic functions of the phylogenetically conserved family of *atg* genes have extensively been studied in yeast.[5,6] One of the most important members of this family is *atg6*, whose mammalian ortholog is represented by the haploinsufficient tumor suppressor gene *beclin 1*.[7,8] In mammalian cells, Beclin 1 acts concertedly with Vps34, Vps15, UVRAG, Bif1, Ambra1 and perhaps other proteins to form a multiprotein complex with class III phosphatidylinositol 3-kinase (PI3K) activity that generates phosphatidylinositol-3-phosphate (PI3P). PI3P determines the curvature of the nascent phagophore and promotes the recruitment of other Atg proteins (including Atg5, Atg12, Atg10, Atg4, Atg3, Atg7, Atg8 and Atg16), which catalyze vesicle elongation and phagophore nucleation.[6,9]

Although classically viewed as an essential mechanism of adaptation to stress, in particular to that imposed by the lack of nutrients, excessive or inefficient autophagy may be involved in autophagic cell death (ACD).[9–11] At a molecular level, the cross-talk between apoptosis and autophagy is beginning to be understood, and some factors have recently been identified as common regulators of both pathways.[9,12,13] For

[1]INSERM, U848, F-94805 Villejuif, France; [2]Institut Gustave Roussy, F-94805 Villejuif, France; [3]Université Paris 11, F-94805 Villejuif, France; [4]Faculty of Chemical and Pharmaceutical Sciences/Medicine, FONDAP Center CEMC, University of Chile, CL-8380492 Santiago, Chile; [5]Mitochondrial Biology Group, Department of Cell and Developmental Biology, University College London, London, WC1E 6BT, UK; [6]Facoltá di Scienze Biotecnologiche, Universitá degli Studi di Napoli Federico II, I-80131 Napoli, Italy and [7]Centre National de la Recherche Scientifique, Institut de Neurobiologie Alfred Fessard, FRC2118, UPR 9040, F-91198 Gif-sur-Yvette, France
*Corresponding authors: G Kroemer, INSERM U848, Institut Gustave Roussy, 39 rue Camille Desmoulins, 94805 Villejuif, France. Tel:+33 1 42 11 60 46; Fax:+33 1 42 11 60 47; E-mail: kroemer@igr.fr or S Lavandero, FONDAP Center CEMC, Faculty of Chemical and Pharmaceutical Sciences, University of Chile, Olivos 1007, 8380492 Santiago, Chile. E-mail: slavander@uchile.cl
[8]These authors share senior co-autorship.
Keywords: apoptosis; Atg genes; autophagic cell death; LC3; lysosomes
Abbreviations: ACD, autophagic cell death; Ambra, activating molecule in Beclin 1-regulated autophagy; Atg, autophagy-related gene; Ca^{2+}, calcium; $[Ca^{2+}]$, Ca^{2+} concentration; $[Ca^{2+}]_c$, cytosolic $[Ca^{2+}]$; CFP, cyan fluorescent protein; cytAEQ, cytosolic aequorin; Cyto, cytosolic; ER, endoplasmic reticulum; FBS, fetal bovine serum; FRET, fluorescence resonance energy transfer; GFP, green fluorescent protein; GFP-LC3, GFP-coupled microtubule-associated protein light chain 3; IMP, inositol monophosphatase ; IP_3, *myo*-inositol 1,4,5-trisphosphate; IP_3R, IP_3 receptor; LBD, ligand-binding domain; mTOR, mammalian target of rapamycin; OMM, outer mitochondrial membrane; PI3K, phosphatidylinositol 3-kinase; PI3P, phosphatidylinositol-3-phosphate; RFP, red fluorescent protein; SERCA, sarco–endoplasmic reticulum Ca^{2+} ATPase; tBHQ, 2,5-di(ter-butyl)-1,4 benzohydroquinone; UVRAG, UV irradiation resistance-associated tumor suppressor gene; Vps, vacuolar protein sorting; YFP, yellow fluorescent protein
Received 14.7.08; revised 25.2.09; accepted 25.2.09; Edited by D Rubinsztein; published online 27.3.09

instance, the activity of Beclin 1 is inhibited by the antiapoptotic proteins Bcl-2 and Bcl-X_L due to the interaction between the BH3 domain present in Beclin 1 and the BH3 receptor cleft of Bcl-2/X_L. This binding is competitively disrupted by proapoptotic BH3-only proteins, which therefore can promote autophagy.[14–16]

Autophagy can also be induced through an mTOR-independent pathway by lowering *myo*-inositol 1,4,5-trisphosphate (IP_3) levels.[17] This effect can be achieved pharmacologically with drugs such as lithium or L-690 330, which disrupt inositol metabolism by inhibiting inositol monophosphatase (IMP).[18] As IP_3 is a second messenger that mediates Ca^{2+} release from the endoplasmic reticulum (ER), autophagy might also be regulated by Ca^{2+}. This hypothesis has been addressed by a pioneering study, which concluded that Ca^{2+} fluxes are not necessary for autophagic stimulation and that autophagy would rather depend on the presence of Ca^{2+} within an intracellular storage compartment.[19] Accordingly, cytosolic Ca^{2+} may even inhibit autophagy in a cyclical mTOR-independent pathway.[18] Three recent studies have also explored the contribution of Ca^{2+} to autophagy,[20–22] establishing that Ca^{2+} is required for autophagic induction, but showing some incongruities in whether increases in cytosolic [Ca^{2+}],[21,22] or modifications of ER Ca^{2+} levels,[20] are responsible for the induction of autophagy. Irrespective of such discrepancies, all these studies showed that a Bcl-2 variant that is specifically targeted to the ER inhibits autophagy.[20,22]

Ca^{2+} present in the ER lumen is released through specific channels. Two types of ER-resident Ca^{2+} release channels exist, namely the ryanodine receptors and the IP_3 receptors (IP_3R).[23] Diverse physiological processes, including the mitochondrial (or intrinsic) pathway of apoptosis, are controlled by Ca^{2+} fluxes from the ER to mitochondria, which occur in the context of specific microdomains allowing for the functional and physical interaction between these organelles.[24,25] The IP_3R plays a critical role in this cross-talk and is currently considered as a major regulator of apoptotic signaling, which is also modulated by the members of the Bcl-2 family of proteins.[24,26–28] The IP_3R has also been shown to regulate autophagy. Indeed, its pharmacological inhibition with xestospongins and its depletion by specific siRNAs, represents a strong stimulus for the induction of autophagy, an effect that can be reverted by ER-targeted Bcl-2 overexpression.[29,30] Moreover, it has been shown that the *IP3R* gene is required for the induction of ACD in *Dyctiostelium discoideum*.[31,32]

On the basis of these pieces of evidence, IP_3R emerges as a possible key integrator of the cross-talk between apoptosis and autophagy. Here, we report that xestospongin B and nutrient starvation disrupt a molecular complex formed by the IP_3R, Beclin 1 and Bcl-2, and present evidence that the IP_3R represses autophagy through Bcl-2-mediated sequestration of Beclin 1.

Results and Discussion

Xestospongin B induces autophagy by binding to the IP_3R in a Bcl-2-inhibitable fashion. The natural compound xestospongin B (purified from the marine sponge *Xestospongia exigua*) is an IP_3R antagonist that induces autophagy when added to a variety of animal cell lines, incuding human cervical adenocarcinoma HeLa cells (Figure 1a–d and Supplementary videos), Rat-1 fibroblasts (from *Rattus norvegicus*; data not shown) and DT40 B-cell lymphoma cells (from *Gallus gallus*; Figure 1d). This was assessed by determining the distribution of green fluorescent protein-coupled microtubule-associated protein light chain 3 (GFP-LC3) to cytoplasmic puncta (Figure 1a and b) or the lipidation of LC3, which leads to an increase in its electrophoretic mobility (from LC3-I to LC3-II; Figure 1c and d). Importantly, these effects were inhibited by overexpression of Bcl-2 (Figure 1a–d) and were lost in DT40 cells depleted for all three IP_3R isoforms through homologous recombination (Figure 1e and f). As a note, DT40 triple knockout cells remained responsive to nutrient starvation as their wild-type counterparts (Figure 1f), suggesting that at least two independent signaling pathways to autophagy – which are activated by distinct triggers – coexist in these cells. As described earlier,[29] xestospongin B caused the dissociation of the Beclin 1/Bcl-2 complex that normally inhibits autophagy. This effect could be detected in coimmunoprecipitation experiments when xestospongin B was added to control DT40 cells, yet was undetectable in IP_3R-deficient DT40 cells (Figure 1g and h).

The redistribution of GFP-LC3 to dots or the accumulation of LC3-II may be a sign of an enhanced formation of autophagosomes or a reduced removal of autophagosomes.[33,34] To discriminate between these two possibilities, we blocked the fusion between autophagosomes and lysosomes (with bafilomycin A1) and/or inhibited lysosomal proteases (with pepstatin A). As an internal control of its efficacy, we ensured that bafilomycin A1 inhibited the colocalization of GFP-LC3 with the lysosomal marker Lamp 2A, which is an indicator of the autophagosome–lysosome fusion (Figure 2a and b). In these conditions, the addition of xestospongin B continued to induce an increase in GFP-LC3 puncta (Figure 2a and c) and in the generation of LC3-II (Figure 2d and e), which strengthens the notion that xestospongin B stimulates the initiation, rather than the late stages, of the autophagic flux.

Xestospongin B neither affected the basal levels nor the histamine-induced increase of IP_3 (Figure 3a). In conditions in which the IMP inhibitor L-690 330 reduced IP_3 levels, non-toxic doses of *myo*-inositol (which lead to an increase in IP_3 concentrations) inhibited L-690 330-induced autophagy, but failed to suppress autophagy induced by xestospongin B (Figure 3b). From these results, we conclude that xestospongin B induces autophagosome formation through a Bcl-2-inhibitable effect on IP_3R that does not involve major perturbations of inositol metabolism.

A molecular complex involving the IP_3R and Beclin 1 regulates autophagy in response to xestospongin B or starvation. Driven by the observation that Bcl-2 overexpression can inhibit xestospongin B-induced autophagy, we monitored the molecular interaction between the IP_3R and Beclin 1, which so far has been indicated as the main target for Bcl-2-mediated autophagy inhibition.[14,15] In unstimulated cells, IP_3R could be immunoprecipitated with

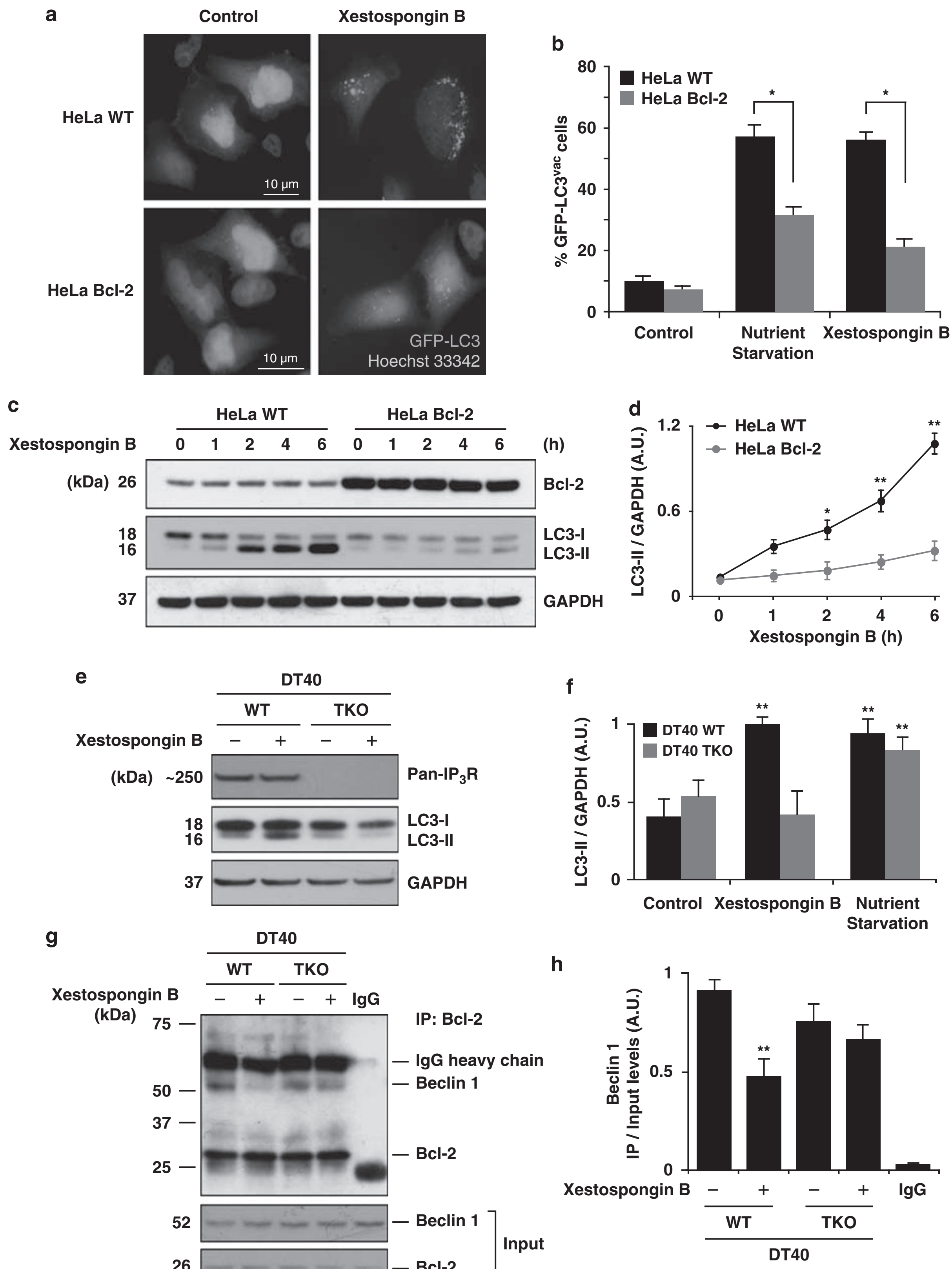
a
Control
Xestospongin B
HeLa WT
HeLa Bcl-2
10 µm
10 µm
GFP-LC3
Hoechst 33342
b
HeLa WT
HeLa Bcl-2
% GFP-LC3vac cells
Control
Nutrient Starvation
Xestospongin B
c
HeLa WT
HeLa Bcl-2
Xestospongin B
(h)
(kDa) 26
Bcl-2
LC3-I
LC3-II
GAPDH
d
HeLa WT
HeLa Bcl-2
LC3-II / GAPDH (A.U.)
Xestospongin B (h)
e
DT40
WT
TKO
Xestospongin B
(kDa) ~250
Pan-IP3R
LC3-I
LC3-II
GAPDH
f
DT40 WT
DT40 TKO
LC3-II / GAPDH (A.U.)
Control
Xestospongin B
Nutrient Starvation
g
DT40
WT
TKO
Xestospongin B
(kDa)
IgG
IP: Bcl-2
IgG heavy chain
Beclin 1
Bcl-2
Beclin 1
Bcl-2
Input
h
Beclin 1 IP / Input levels (A.U.)
Xestospongin B
IgG
WT
TKO
DT40

Beclin 1 and *vice versa*. Shortly after addition of xestospongin B (usually within 3 h), this interaction was reduced (Figure 4a and b). As described earlier by our group, xestospongin B disrupted the interaction between Beclin 1 and Bcl-2,[29] whereas it did not affect the co-immunoprecipitation between the IP_3R and Bcl-2 (Figure 4c). This suggests that xestospongin B disrupts the interaction between Beclin 1 and the IP_3R/Bcl-2 complex. Similar results were found when xestospongin B treatment was replaced by the most physiological inducer of autophagy, nutrient starvation (Figure 4d), and could also be detected in different cell lines, including human colon cancer HCT116 cells and Rat-1 fibroblasts (not shown). In cells that overexpress Bcl-2, the capacity of xestospongin B to disrupt the IP_3R/Beclin 1 complex was reduced and delayed (Figure 4e). Importantly, when Bcl-2 was depleted by specific siRNAs (Figure 4f), the IP_3R/Beclin 1 complex was disrupted in resting conditions (Figure 4g), further corroborating the notion that the interaction between IP_3R and Beclin 1 is mediated by Bcl-2. Although mTOR phosphorylation and mTOR-mediated phosphorylation of $p70^{S6K}$ were inhibited by rapamycin, xestospongin B did not affect mTOR phosphorylation or $p70^{S6K}$ phosphorylation (Figure 5a). Moreover, mTOR inhibition with rapamycin, which induces autophagy, failed to disrupt the IP_3R/Beclin 1 complex (Figure 5b). Altogether, these results strongly suggest that the inhibition of mTOR and that of the IP_3R induce autophagy through mechanisms that can be fully separated.

As several IP_3R-interacting proteins, including Bcl-2, have major effects on Ca^{2+} signaling,[27] we tested whether Beclin 1 might also affect Ca^{2+} homeostasis, which reportedly has an important impact on autophagy.[18–22] However, we did not detect any tangible effect of Beclin 1 depletion on IP_3R agonist-induced Ca^{2+} fluxes (Figure 6a and b), steady state levels of Ca^{2+} in the ER lumen, thapsigargin-induced Ca^{2+} depletion from the ER (Figure 6c), or increases in cytosolic $[Ca^{2+}]$ upon inhibition of the sarco–ER Ca^{2+} ATPase (SERCA) with 2,5-di(ter-butyl)-1,4 benzohydroquinone (tBHQ; Figure 6d and e). This was assessed by using state-of-the-art aequorin-based Ca^{2+} sensors (Figure 6a and b), ERD1 cameleon Ca^{2+} sensor (Figure 6c) or a chemical Ca^{2+} probe (Figure 6d and e). Collectively, these data indicate that the IP_3R can affect the autophagy-inducing function of Beclin 1, yet suggest that Beclin 1 itself does not play a major role in regulating Ca^{2+} fluxes governed by the IP_3R.

The IP_3R ligand-binding domain (IP_3R-LBD) inhibits autophagy through an effect on the Beclin 1/Bcl-2 complex. A target for xestospongin B is the IP_3R-LBD (aa 224–604), which is engaged in several protein–protein interactions;[35,36] and has a major effect on the regulation of ER-mitochondrial microdomains that affect Ca^{2+} signaling and the physical contact between ER and mitochondria.[24] The transfection-enforced expression of the IP_3R-LBD coupled to red fluorescent protein (RFP) strongly inhibited autophagy induced by xestospongin B or nutrient starvation (Figure 7a and b). This held so for either ER-targeted, outer mitochondrial membrane (OMM)-targeted and cytosolic (Cyto) variants of the IP_3R-LBD coupled to RFP, all of which affect the ER–mitochondrial cross-talk.[24] As negative controls, equally targeted versions of RFP (namely Cyto-ER- and OMM-RFP) failed to inhibit autophagy in this system, as assessed by measuring GFP-LC3 puncta (Figure 7a and b) or the accumulation of LC3-II (Figure 7e). Moreover, an inactive IP_3R-LBD mutant (IP_3R-LBD-9aaER-RFP) in which the insertion of a nonapeptide linker abolishes the interaction with endogenous IP_3R,[37] failed to affect xestospongin B-induced autophagy (Figure 7b). All the functional variants of the IP_3R-LBD-RFP (Cyto-, OMM- and ER-targeted) but not IP_3R-LBD-9aaER-RFP, interacted with Beclin 1 (not shown), and this interaction was reduced in the ER by depletion of Bcl-2 (Figure 7c and d). Altogether, these results indicate that IP_3R-LBD is the moiety of the IP_3R that mediates its interaction with Beclin 1 (through Bcl-2), and accounts for IP_3R-mediated inhibition of autophagy.

Conclusions

The results from this and several earlier studies,[17,18,29,30] indicate that IP_3R agonists (such as IP_3 itself) and IP_3R antagonists (such as xestospongins) act as inhibitors and inducers of autophagy, respectively, through an effect on the IP_3R. Thus, xestospongin B, which reportedly competes with IP_3 for IP_3R binding,[38,39] induces autophagy through the IP_3R (in the sense that this effect is lost in IP_3R knockout cells) rather than through an off-target effect. Although acute depletion of the IP_3R by RNA interference is sufficient to induce autophagy in HeLa cells,[29] permanent IP_3R knockout by homologous recombination does not induce autophagy, at least in DT40 cells, presumably because these cells have adapted to the absence of the IP_3R in a long-term selection process and express a truncated version of IP_3R.[40] Conversely, plasmid-driven overexpression of the IP_3R-LBD inhibits autophagic vacuolization induced by both xestospongin and nutrient starvation, further confirming the major impact of the IP_3R on the regulation of autophagy.

Although accumulating evidence point to the modulation of autophagy by the IP_3R, the underlying mechanisms are still

Figure 1 Induction of autophagy by xestospongin B is dependent on the IP_3R and Bcl-2. Bcl-2 inhibits xestospongin B-induced autophagy (**a**–**d**). Wild-type (WT) or Bcl-2 overexpressing HeLa cells transfected with GFP-LC3 were treated with xestospongin B (2 μM) for 4 h. Autophagy was monitored by assessing the intracellular redistribution of GFP-LC3 (**a**), and the percentage of vacuolizated cells was quantified (**b**). LC3 lipidation was compared between WT and Bcl-2 overexpressing HeLa cells by immunoblotting (**c**), and quantified (**d**) at the times indicated. The IP_3R was necessary for xestospongin B-(4 h), but not starvation-mediated (2 h) LC3 lipidation, as observed in WT DT40 chicken B lymphocytes *versus* a triple knockout (TKO) DT40 cell line deficient for all IP_3R isoforms (**e** and **f**). Bcl-2 and Beclin 1 interaction was monitored after 6 h of xestospongin B treatment in WT *versus* TKO DT40 cells (**g**), and the coimmunoprecipitated levels of Beclin 1 were normalized to input levels (**h**). Results are representative of at least three independent experiments. $^{*}P<0.05$ and $^{**}P<0.01$ as indicated for WT compared with genetically modified cells. The colour reproduction of this figure is available on the html full version of the manuscript

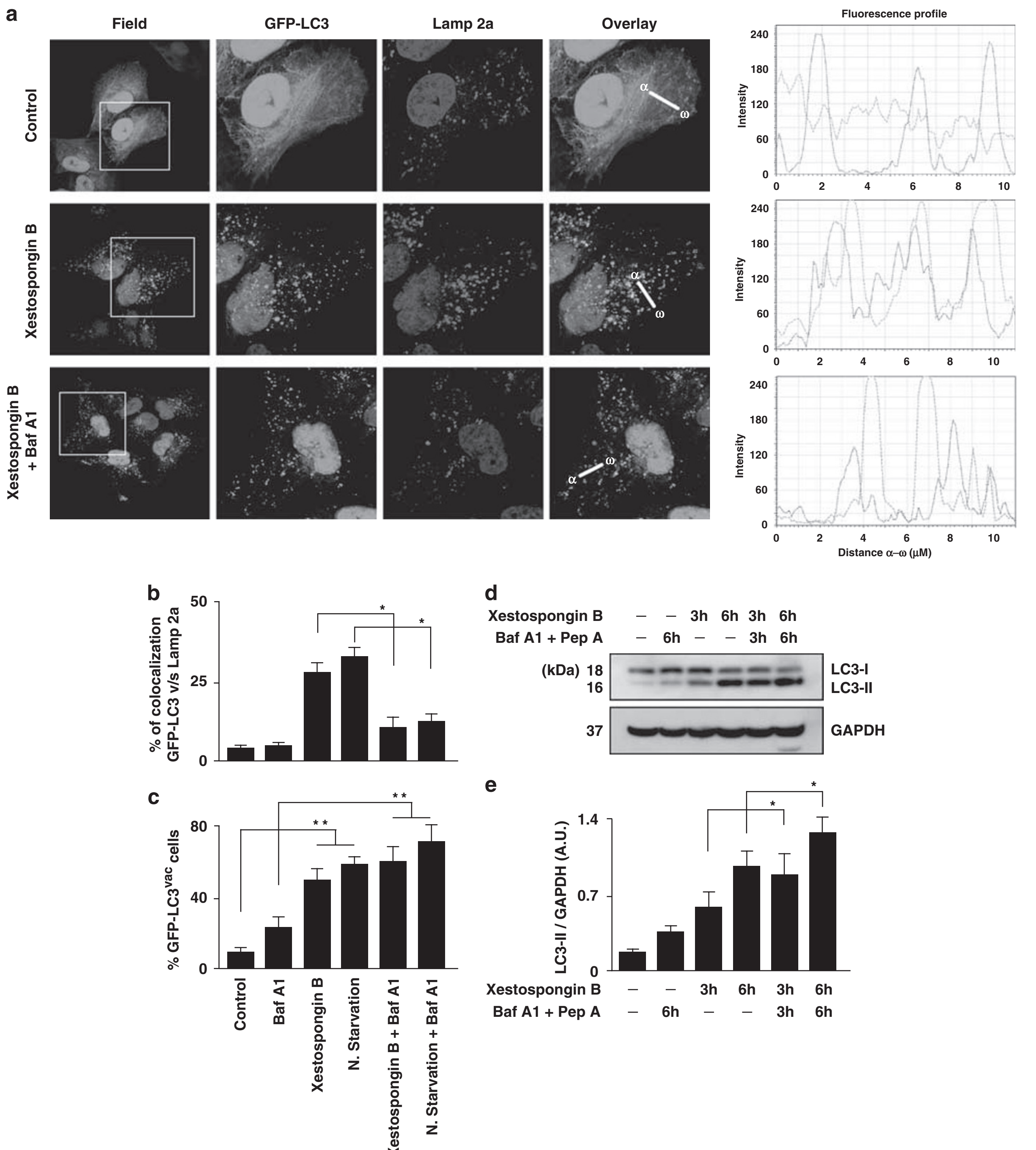

Figure 2 On-rate autophagic flux induced by xestospongin B. HeLa cells transiently expressing GFP-LC3 were preincubated (30 min) with bafilomycin A1 and then subjected to xestospongin B treatment (4 h) or to nutrient starvation (2 h). Confocal images were acquired, the degree of colocalization between GFP-LC3 and the lysosomal marker Lamp 2a was quantified (**a** and **b**), and the percentage of cells with GFP-LC3 puncta was determined (**c**). A mixture of bafilomycin A1 (1 nM) and pepstatin A1 (10 μg/ml) was employed to inhibit the lysosomal degradation of LC3-II (**d**). LC3-II relative to GAPDH levels were quantified (**e**). $^{*}P<0.05$; $^{**}P<0.01$ as indicated. The colour reproduction of this figure is available on the html full version of the manuscript

unclear. IP_3R controls the agonist-induced release of Ca^{2+} from the ER lumen to the cytosol,[35] and elevations of cytosolic Ca^{2+} have been involved in pharmacologically induced autophagy, as occurred in response to vitamin D analogs.[22] Hence, the finding that IP_3R inhibition with xestospongins induces autophagy (although it should reduce[39] cytosolic Ca^{2+}) suggests that the effects of the IP_3R and/or IP_3R ligands on autophagy cannot be explained only by a modulation of Ca^{2+} levels. Here, we show that the IP_3R coimmunoprecipitates with Beclin 1, suggesting another

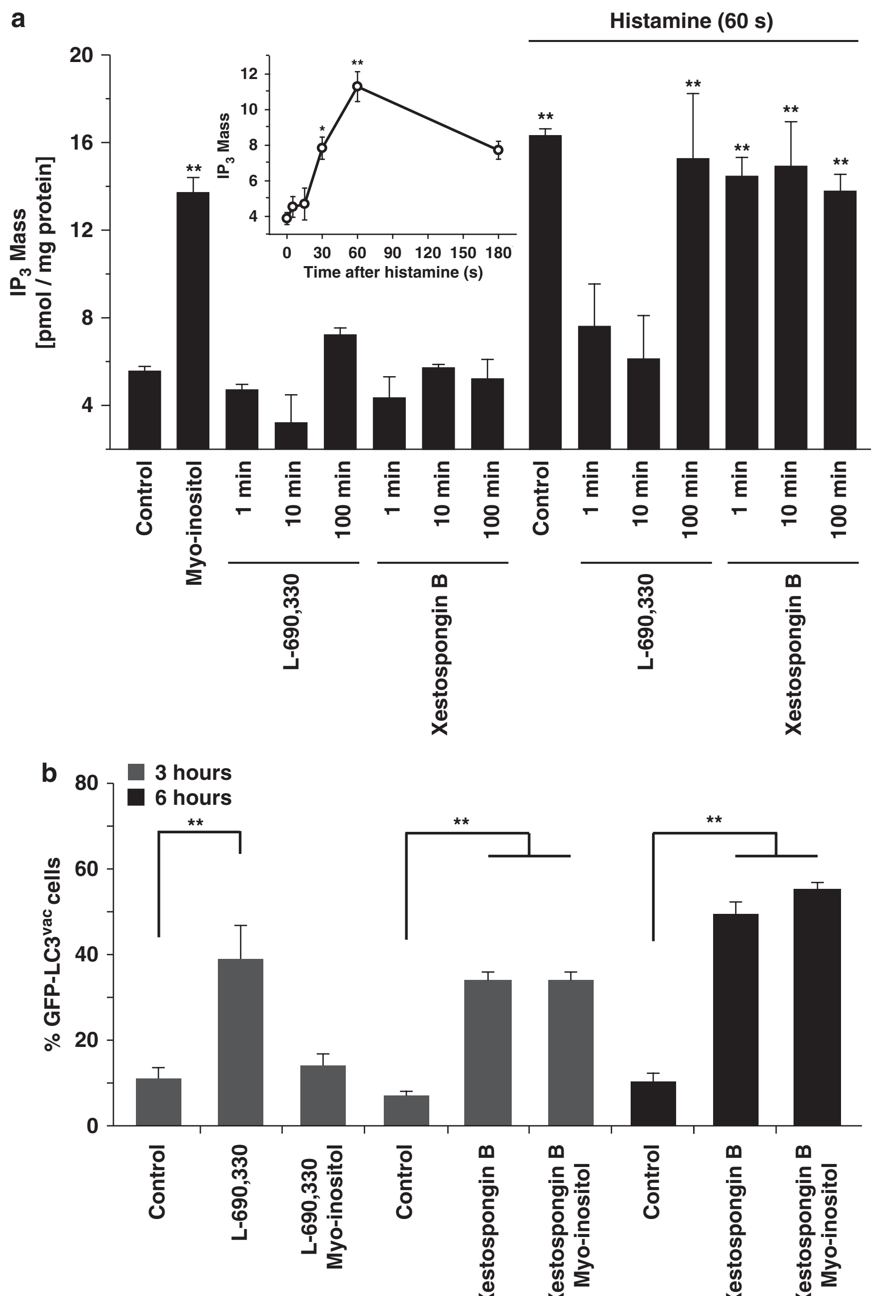

Figure 3 Autophagy induced by xestospongin B is IP_3-independent. Intracellular levels of the transient messenger IP_3 were measured with a radioreceptor assay under basal or histamine-induced peak conditions (**a**). The inset graphic depicts a typical time-response to identify the time of IP_3 peak concentrations, as induced by histamine (100 μM) stimulation. Treatment with *myo*-inositol (10 μM, 10 min), L-690 330 (100 μM) and xestospongin B (2 μM) were compared under basal as well as peak conditions evoked by histamine (**a**). HeLa cells transiently expressing GFP-LC3 were treated with xestospongin B in the presence or absence of *myo*-inositol. The percentage of vacuolizated cells was determined at the indicated times (**b**). Data are presented as mean ± S.E.M. of three independent triplicates. *$P < 0.05$ and **$P < 0.01$ *versus* unstimulated control (**a**) or as indicated (**b**)

mechanism through which the IP_3R might act as an endogenous inhibitor of autophagy. Indeed, we found that IP_3R binding by its antagonist xestospongin B, as well as physiological induction of autophagy by nutrient starvation, disrupted the interaction between the IP_3R and Beclin 1. As this interaction was abolished by the knockdown of Bcl-2, it is likely that the IP_3R and Beclin 1 interact through an indirect link established by Bcl-2.

In the triangular game among the IP_3R, Beclin 1 and Bcl-2, the IP_3R-LBD (which is the site of interaction with IP_3 and xestospongins) appears as the most important domain for the regulation of autophagy. Thus, the IP_3R-LBD (which itself has no function as a Ca^{2+} channel)[41] can inhibit autophagy irrespective of its precise subcellular localization or topology, once more arguing against the idea that modified Ca^{2+} fluxes account for the effects of IP_3R on autophagy. We were unable

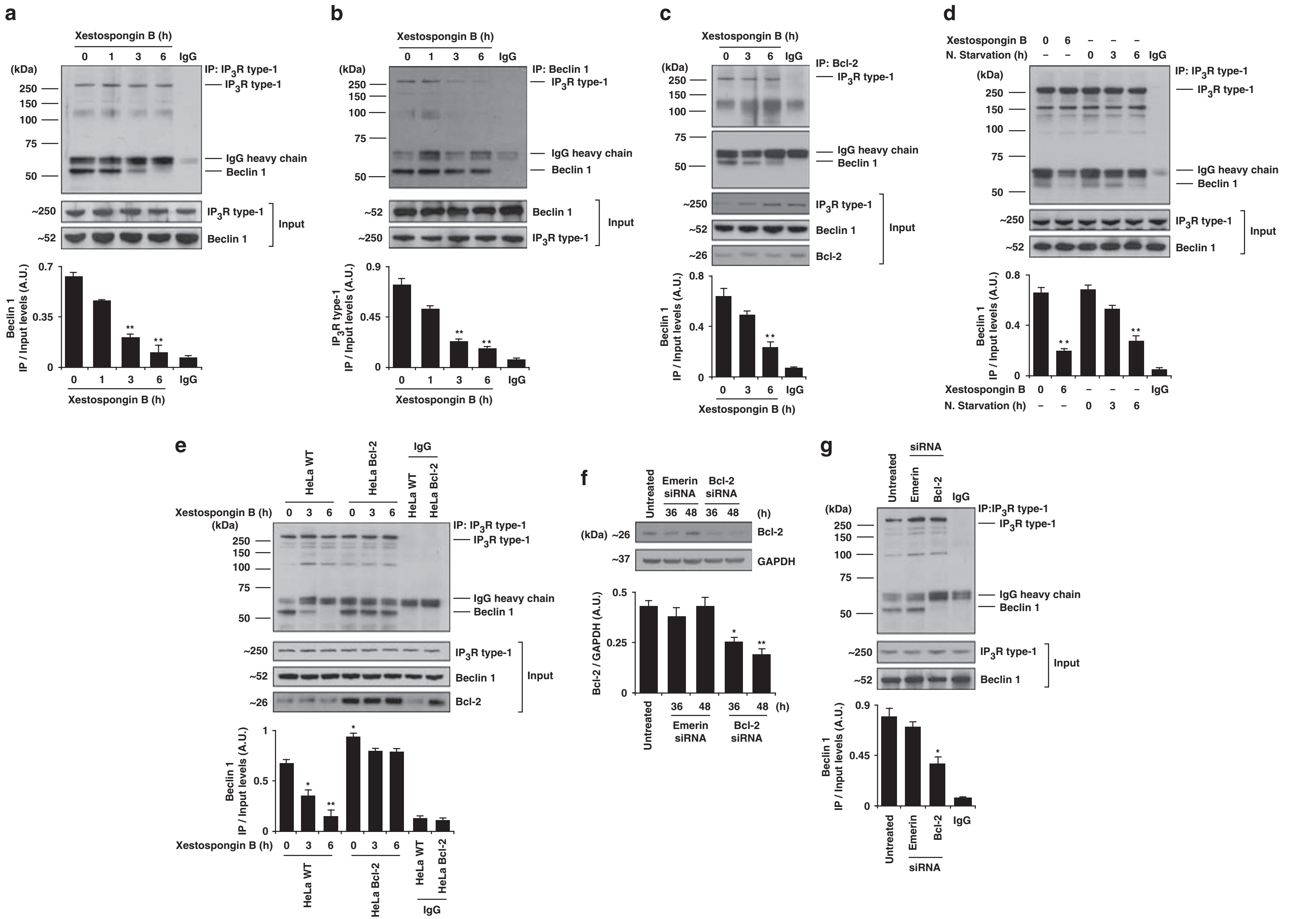

Figure 4 A Bcl-2-dependent molecular complex comprising the IP_3R and Beclin 1 regulates autophagy. Immunoprecipitation assays were carried out as indicated in Materials and Methods using wild-type (WT) (**a**–**d**) and Bcl-2 overexpressing HeLa cells (**e**), as well as HeLa cells in which Bcl-2 was depleted by specific siRNAs (**g**). Xestospongin B induces the dissociation of Beclin 1 from the IP_3R (**a**) and vice versa (**b**), as well as the separation of Beclin-1 from Bcl-2, without affecting the interaction between the IP_3R and Bcl-2 (**c**). Under nutrient starvation conditions, the interaction between Beclin 1 and the IP_3R was also lost (**d**). In HeLa cells, stably overexpressing Bcl-2, the xestospongin B-mediated dissociation of Beclin 1 from the IP_3R was reduced, compared with WT HeLa cells (**e**). Conversely, in HeLa cells depleted of Bcl-2 (**f**), the interaction between Beclin 1 and the IP_3R was already lost in unstimulated conditions (**g**). In all experiments, coimmunoprecipitated protein levels were quantified relative to input protein levels. Data are presented as mean ± S.E.M. of three independent triplicate assessments. $^{*}P<0.05$ and $^{**}P<0.01$ *versus* untreated controls

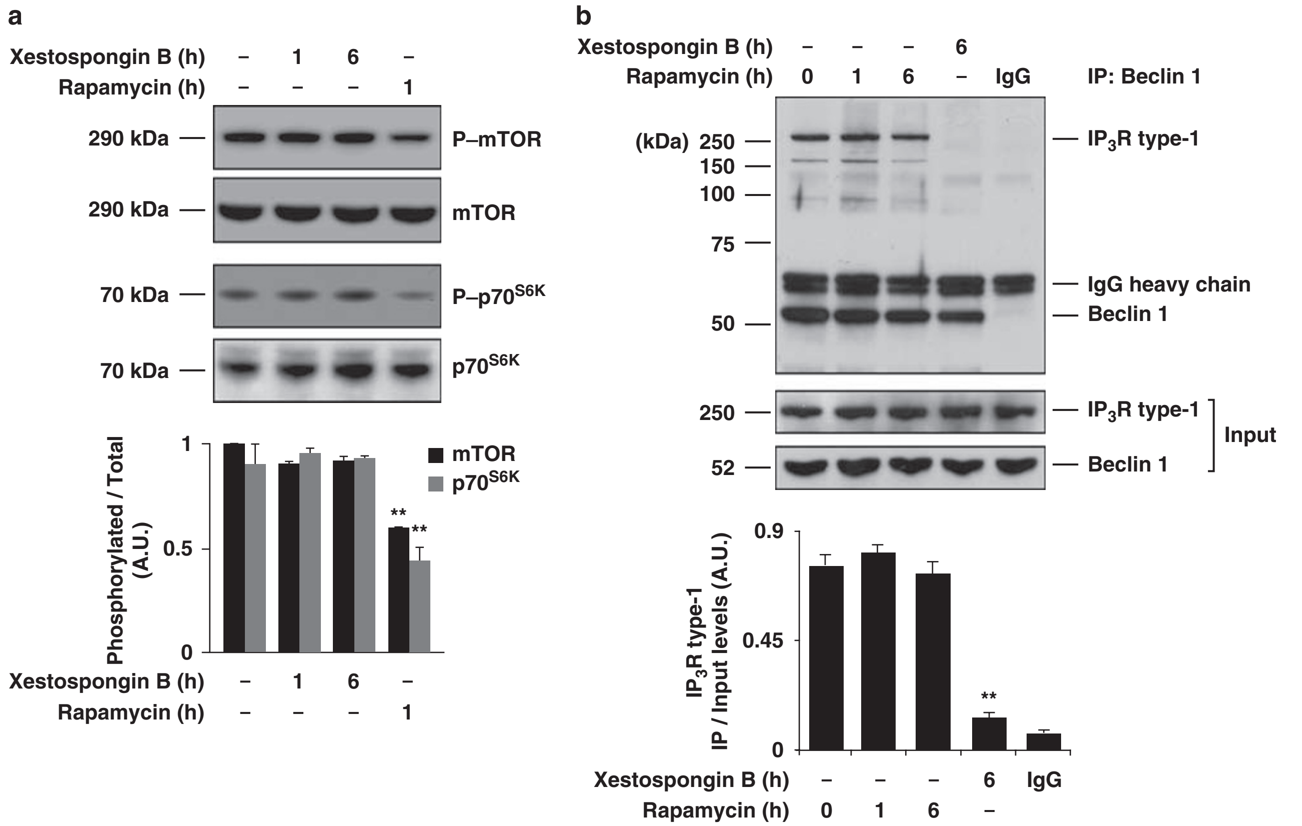

Figure 5 Xestospongin B effects are mTOR-independent. HeLa cells were treated with xestospongin B (2 μM) or rapamycin (1 μM) for the indicated periods and the levels of mTOR and $p70^{S6K}$ phosphorylation were assessed by immunoblotting (**a**). The Beclin 1/IP_3R interaction was not modified by rapamycin treatment, in conditions in which xestospongin B caused its dissociation (**b**). Results are presented as mean ± S.E.M. of three independent triplicate assessments. $^{**}P<0.01$ *versus* untreated controls

to detect any effects of Beclin 1 knockdown on Ca^{2+} fluxes at the ER membrane, which suggests that Beclin 1 affects autophagy regulation mainly as an allosteric regulator of Vps34 (and perhaps other yet-to-be-discovered enzymatic activities and molecular motors), rather than through gross effects on Ca^{2+} handling.

In synthesis, the results contained in this study identify the IP_3R as a new, unsuspected regulator of the Beclin 1 complex that bridges signals converging on the ER and initial phagophore formation. Although the molecular details of this cross-talk require further exploration, our data point to the presence of an intriguing regulatory network in which the conformation of the IP_3R, as influenced by agonists and/or antagonists acting on its LBD, regulates the initiation of autophagy through an effect on Beclin 1.

Materials and Methods

Cells and treatments. Wild-type, Bcl-2 overexpressing and GFP-LC3 overexpressing derivatives of the human cervix adenocarcinoma HeLa cell line, as well as the rat fibroblast cell line Rat-1, were grown in Glutamax-containing Dulbecco's modified Eagle's medium supplemented with 10% heat-inactivated fetal bovine serum (FBS) and 10 mM HEPES buffer. Wild-type and IP_3R-triple deficient chicken lymphoma DT40 cells were maintained in Glutamax-containing RPMI 1640 medium supplemented with 10% FBS, 1% chicken serum, 10 mM HEPES buffer and 10 μM 2-mercaptoethanol. All cell lines were cultured in the presence of 100 U/ml penicillin G and 100 μg/ml streptomycin, at 37 °C (5%) CO_2. All media and supplements for cell culture were purchased from Gibco-Invitrogen (Carlsbad, USA). For serum and amino-acid starvation, cells were cultured in serum-free Earle's Balanced Salt Solution medium (Sigma-Aldrich, St. Louis, MO, USA), a condition that we refer to as 'nutrient starvation'. All cell lines were seeded in 6-, 12- or 24-well plates and grown for 24 h before treatments. Unless otherwise indicated, chemicals were purchased from Sigma-Aldrich. Bafilomycin A1 (1 nM), histamine (1–100 μM), L-690 330 (100 μM; Tocris, Bristol, UK), *myo*-inositol (10 μM; Calbiochem, Darmstadt, Germany), pepstatin A (10 μg/ml) and xestospongin B (2 μM, extracted from the marine sponge *Xestospongia exigua* as described earlier[38,42]) were added for 0–8 h, as indicated.

Dynamic *in vivo* [Ca^{2+}] measurements. Basal and 2,5-di(ter-butyl)-1,4 benzohydroquinone (tBHQ)- or histamine-induced cytosolic Ca^{2+} signals were measured using either Fura-2 or the cytosolic version of the recombinant Ca^{2+} sensor aequorin (cytAEQ). All measurements were carried out in Krebs–Ringer modified buffer (KRB): 135 mM NaCl, 5 mM KCl, 1 mM $MgSO_4$, 0.4 mM K_2HPO_4, 5.5 mM glucose, 20 mM HEPES (pH = 7.4), supplemented with 1 mM $CaCl_2$. HeLa cells were loaded with 3 μM Fura-2/AM in KRB for 20 min at 37 °C and 10 min at RT. Cells were then perfused with KRB followed by 100 μM tBHQ, and dye calibration was performed using ionomycin (1 μM, the highest peak value) and ionomycin/EDTA (1 μM/1 mM, the lowest peak value). Changes in emission at 520 nm after sequential excitation at 340 and 380 nm were recorded and calibrated into $[Ca^{2+}]_c$ from the ratio of emitted fluorescence, on the basis of an earlier described procedure that used a dissociation constant of 224 nM for Fura-2.[43] HeLa cells transiently expressing cytAEQ were administrated with coelenterazine and transferred to a perfusion chamber. The light signal was collected in a purpose-built luminometer and calibrated into $[Ca^{2+}]_c$ values as described earlier.[44] To quantify the Ca^{2+} content of the ER, the fluorescence resonance energy transfer (FRET)-based ER-targeted ERD1 probe[45] was imaged using a Zeiss LSM 510 Meta laser confocal system (Carl Zeiss AG, Oberkochen, Germany). The probe was excited by a 405 nm laser diode, emission spectra were acquired at 420–600 nm and the yellow fluorescent protein (YFP) and cyan fluorescent protein (CFP) signals were obtained by unmixing the spectrum on the basis of previously registered

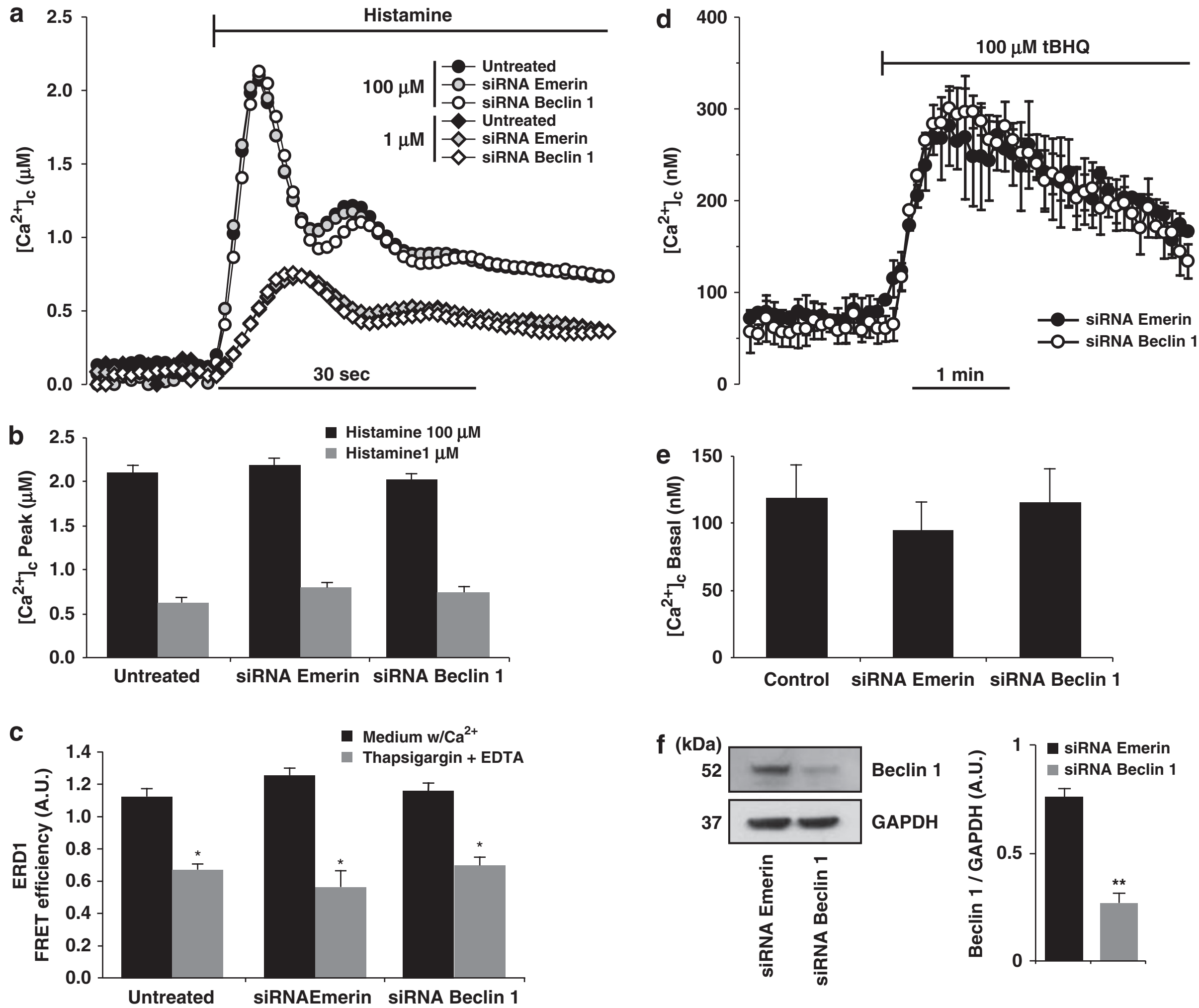

Figure 6 Beclin 1 depletion does not affect Ca^{2+} homeostasis. HeLa cells were transfected with specific siRNAs targeting Beclin 1 or the unrelated protein emerin. After 48 h, cells were subjected to $[Ca^{2+}]$ measurements (**a**–**e**) or immunoblotting to check Beclin 1 levels (**f**). Histamine-evoked (1 and 100 μM) cytosolic $[Ca^{2+}]$ increases were measured using cytAEQ. Representative traces (**a**) and mean ± S.E.M. peak values are shown for each condition (**b**). Steady-state ER Ca^{2+} levels and thapsigargin-induced ER Ca^{2+} depletion levels were measured with the FRET probe ERD1 and mean ± S.E.M. values are shown (**c**). Cytosolic $[Ca^{2+}]$ after ER depletion with tBHQ (**d**), as well as steady-state cytosolic Ca^{2+} levels (**e**) were quantified using Fura-2. Representative traces and mean values ± S.E.M. are shown, respectively. *$P<0.05$ *versus* culture medium with Ca^{2+}. **$P<0.01$

spectra of separate CFP and YFP proteins, as well as the autofluorescence of non-transfected cells. FRET efficiency, which is a function of ER luminal $[Ca^{2+}]$, was quantified using the acceptor bleaching method.[45] Briefly, after five acquisitions, YFP was bleached (at both 488 and 514 nm excitation wavelengths, typically by about 80–90%), followed by acquisition of further five image spectra. Reduction of the YFP signal leads to an increase in the CFP signal, which is normalized to the decrease of YFP intensity during bleaching. The normalized increase of CFP intensity is presented as FRET efficiency.

Immunoblots and immunoprecipitation. All cell lines (4×10^6 cells) were washed with PBS and lysed as describe earlier.[46] For immunoblotting, 50 μg of protein were separated onto NuPAGE gels (Invitrogen) and transferred to Immobilion-P^{SQ} PVDF membranes (Millipore Corporation, Billerica, MA, USA). Membranes were incubated for 1 h in PBS-Tween 20 (0.05%) containing 5% BSA. Primary antibodies specific for Bcl-2, Beclin 1 (Santa Cruz Biotechnology, Santa Cruz, CA, USA), IP_3R-I (Calbiochem), IP_3R types I-II-III (Santa Cruz), LC3B, mTOR, $p70^{S6K}$, phospho-mTOR or phospho-$p70^{S6K}$ (Cell Signaling, Danvers, MA, USA) were incubated overnight at 4 °C and revealed with the appropriate horseradish peroxidase-labeled secondary antibodies (SouthernBiotech, Birmingham, AL, USA) by means of the SuperSignal West Pico chemoluminiscent substrate (Pierce, Rockford, IL, USA). An antibody recognizing GAPDH (Chemicon) was used to control equal loading of lanes. For immunoprecipitation, extracts from HeLa cells (8×10^6 cells) were lysed and 400 μg of protein were precleared for 1 h with 15 μl of Protein G Sepharose 4 Fast Flow (GE Healthcare, Piscataway, NJ, USA), and subsequently incubated for 3 h in the presence of anti-Beclin 1 antibody, anti-IP_3R-I, anti-RFP (Abcam, Cambridge, UK) and anti-Bcl-2 or immunoglobulin control. Immunoprecipitation immunoblotting was carried out using TrueBlot-HRP (eBioscience, San Diego, CA, USA) secondary antibodies. Quantitative analysis of immunoblots was carried out by using the open source ImageJ software (freely available at http://rsbweb.nih.gov/ij/index.html). Results are presented as mean ± S.E.M. Three independent experiments were carried out in triplicate, and statistical significance was evaluated by Student's *t*-test.

Immunofluorescence microscopy. For immunofluorescence staining, cells were fixed with paraformaldehyde (4% w/v, 20 min), permeabilized with Triton X-100 (0.3% in PBS, 30 min), blocked with 3% BSA and incubated overnight at 4°C with a specific antibody against Lamp 2a (200 ng/ml; Santa Cruz). Nuclei were counterstained with 10 μg/ml Hoechst 33342 (Molecular Probes-Invitrogen, Carlsbad, CA, USA). Conventional fluorescence microscopy was performed with a Leica IRE2 microscope equipped with a DC300F camera (Leica Microsystems,

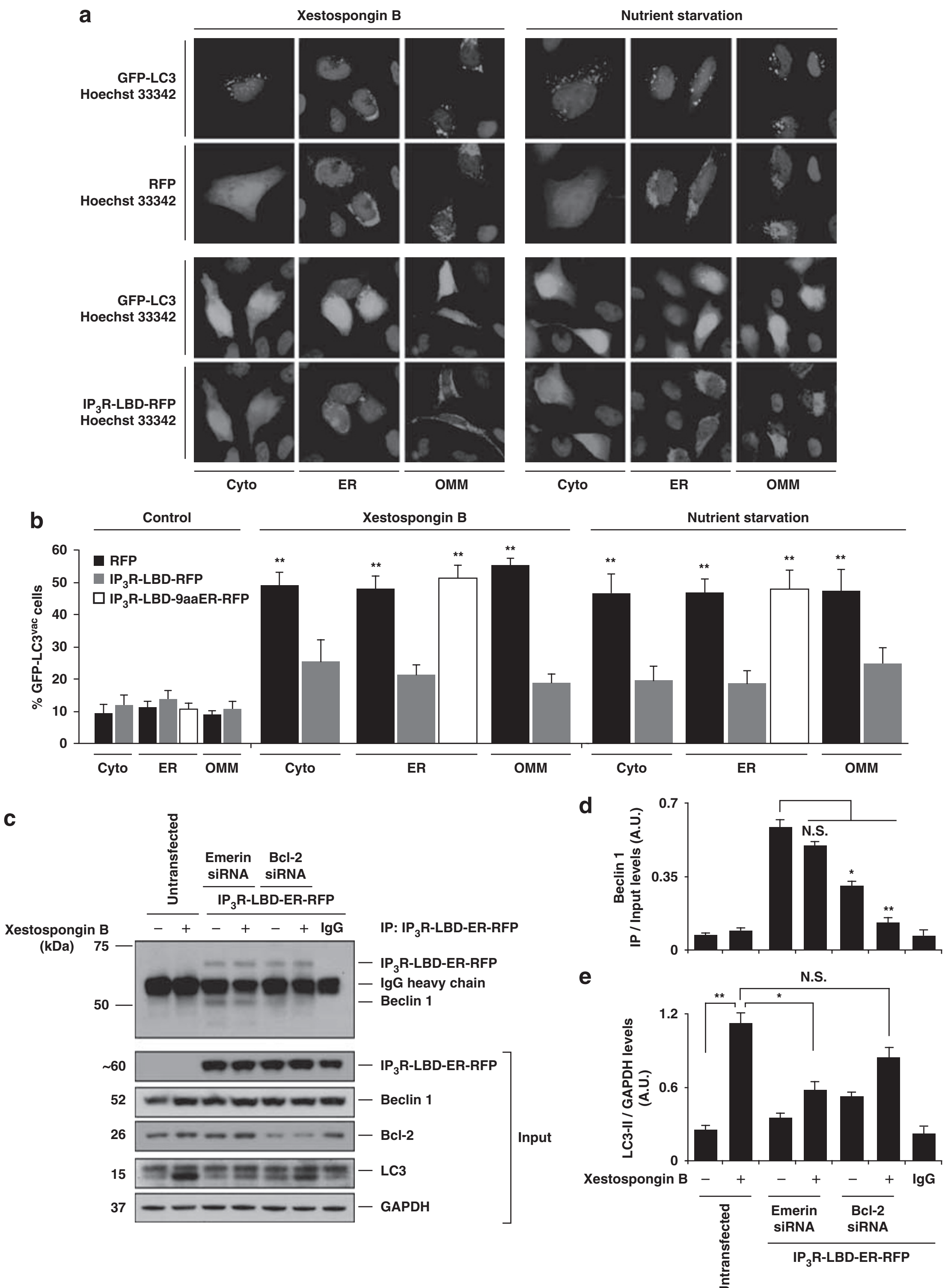

Figure 7 Overexpression of the IP_3R-LBD inhibits xestospongin B-induced autophagy through interaction with Beclin 1. HeLa cells were cotransfected with GFP-LC3 and three IP_3R-LBD-RFP chimeric proteins targeted to different subcellular compartments, namely the cytosol (Cyto), the outer mitochondrial membrane (OMM) and the endoplasmic reticulum (ER). An inactive ER-targeted IP_3R-LBD-RFP, including a non-apeptide linker (9aaER) as well as equally targeted variants of RFP alone were used as controls. Twenty-four hours after transfection, cells were subjected to treatment with xestospongin B or nutrient starvation. Representative pictures of Hoechst 33342-counterstained cells were taken 4 h after treatment (**a**) and the percentage of adherent cells exhibiting GFP-LC3 vacuolization into cytoplasmic puncta was determined (**b**). The interaction between the IP_3R-LBD and Beclin 1 was assessed by immunoprecipitation experiments in HeLa cells that were transiently expressing IP_3R-LBD-ER-RFP and concomitantly subjected to siRNA-mediated emerin or Bcl-2 knockdown as indicated (**c**). Coimmunoprecipitated Beclin 1 levels were normalized relative to input protein levels (**d**). LC3-II levels from the input lysates were normalized relative to GAPDH levels (**e**). Data are reported as mean ± S.E.M. of three independent experiments carried out in triplicates. $^{*}P<0.05$ and $^{**}P<0.01$. The colour reproduction of this figure is available on the html full version of the manuscript

Wetzlar, Germany). Confocal microscopy was carried out with a Leica TSC-SPE microscope equipped with a $63 \times /1.15$ Olympus objective by using LAS software (Leica Microsystems). Cells presenting a diffuse distribution of GFP-LC3 in the cytoplasm and nucleus were considered as non-autophagic, whereas cells exhibiting both several intense punctuate GFP-LC3 aggregates and nuclear GFP-LC3 exclusion were classified as autophagic (GFP-$LC3^{vac}$). Each GFP-LC3 staining was independently quantified by two investigators (JMV and CO).

Measurement of intracellular IP_3 levels. HeLa cells (4×10^6) were seeded in 100 mm culture dishes and were incubated after 24 h with L-690 330 (100 μM), *myo*-inositol (10 μM) and/or xestospongin B (2 μM) for 0–100 min. Immediately afterwards, they were stimulated with histamine (100 μM) for 0–3 min and lysed with 0.2 M ice-cold trichloroacetic acid. Cell extracts were then subjected to a radioreceptor assay (Perkin Elmer no. NEK064, Waltham, MA, USA). IP_3 levels were quantified in a liquid scintillation counter (Packard Tri-carb 2100TR, Packard Instrument, Meriden, CT, USA) and normalized to the amount of protein contained in each sample. Results are presented as mean $\pm$ S.E.M. Three independent experiments were carried out in triplicate and statistical significance was evaluated by Student's *t*-test.

Plasmids, transfection and RNA interference. Cells were cultured in 6-well plates and transfected at 80% confluence by using Oligofectamine reagent (Invitrogen), with small interfering RNAs (siRNAs) specifically targeting human Beclin 1 (sense 5′-GAUUGAAGACACAGGAGGC-3),[47,48] Bcl-2 (sense 5′-GCUGCACCUGACGCCCUUCTT-3′)[47,49] or the unrelated protein emerin (sense 5′-TATGTCCTCCTCATCATCTTCCT-3′).[50] All siRNAs were purchased from Sigma-Proligo. Transient transfections with plasmids were carried out with Lipofectamine 2000 reagent (Invitrogen) and cells were used 24 h after transfection. Cells were transfected with an empty control vector or with a plasmid encoding for GFP-LC3.[51] Cotransfection was carried out using a mixture of the GFP-LC3-encoding plasmid and plasmids encoding for variants of the IP_3R-LBD coupled to RFP targeted to different subcellular compartments, namely the cytosol (IP_3R-LBD-RFP-Cyto), the OMM (IP_3R-LBD-RFP-OMM) and the ER (IP_3R-LBD-RFP-ER). As controls, a plasmid coding for an ER-targeted IP_3R-LBD that is rendered inactive by the incorporation of a nonapeptide linker sequence (IP_3R-9aa-LBD-RFP-ER), as well as plasmids encoding RFP alone targeted to the cytosol (RFP-Cyto), the OMM (RFP-OMM) or the ER (RFP-ER) were used.[24,37,52]

Acknowledgements. GK is supported by the Ligue Nationale contre le Cancer (équipe labellisée), European Commission (RIGHT, ChemoRes, Apop-Train, Apo-SYs), Agence Nationale pour la Recherche, Cancéropôle Ile-de-France and Institut National contre le Cancer (INCa). We thank the International Collaboration Program ECOS-CONICYT, project C08S01. JMV is supported by Fondation pour la Recherche Médicale and CONICYT. CO holds a PhD scholarship from CONICYT, Chile. OK is supported by EMBO. AWEJ is a Medical Research Council student. We also thank Michael R Duchen (University College London) for the use of confocal facility (Zeiss LSM 510 Meta) and discussions, as well as to Dr. Roger Y Tsien (University of California at San Diego) for the donation of ERD1.

1. Klionsky DJ. Autophagy: from phenomenology to molecular understanding in less than a decade. *Nat Rev Mol Cell Biol* 2007; **8**: 931–937.
2. Klionsky DJ, Emr SD. Autophagy as a regulated pathway of cellular degradation. *Science* 2000; **290**: 1717–1721.
3. Yorimitsu T, Klionsky DJ. Autophagy: molecular machinery for self-eating. *Cell Death Differ* 2005; **12** (Suppl 2): 1542–1552.
4. Rubinsztein DC, Gestwicki JE, Murphy LO, Klionsky DJ. Potential therapeutic applications of autophagy. *Nat Rev Drug Discov* 2007; **6**: 304–312.
5. Klionsky DJ, Cregg JM, Dunn Jr WA, Emr SD, Sakai Y, Sandoval IV *et al.* A unified nomenclature for yeast autophagy-related genes. *Dev Cell* 2003; **5**: 539–545.
6. Xie Z, Klionsky DJ. Autophagosome formation: core machinery and adaptations. *Nat Cell Biol* 2007; **9**: 1102–1109.
7. Aita VM, Liang XH, Murty VV, Pincus DL, Yu W, Cayanis E *et al.* Cloning and genomic organization of beclin 1, a candidate tumor suppressor gene on chromosome 17q21. *Genomics* 1999; **59**: 59–65.
8. Yue Z, Jin S, Yang C, Levine AJ, Heintz N. Beclin 1, an autophagy gene essential for early embryonic development, is a haploinsufficient tumor suppressor. *Proc Natl Acad Sci USA* 2003; **100**: 15077–15082.
9. Galluzzi L, Vicencio JM, Kepp O, Tasdemir E, Maiuri MC, Kroemer G. To die or not to die: that is the autophagic question. *Curr Mol Med* 2008; **8**: 78–91.
10. Galluzzi L, Maiuri MC, Vitale I, Zischka H, Castedo M, Zitvogel L *et al.* Cell death modalities: classification and pathophysiological implications. *Cell Death Differ* 2007; **14**: 1237–1243.
11. Kroemer G, Galluzzi L, Vandenabeele P, Abrams J, Alnemri ES, Baehrecke EH *et al.* Classification of cell death: recommendations of the Nomenclature Committee on Cell Death 2009. *Cell Death Differ* 2009; **16**: 3–11.
12. Levine B, Sinha S, Kroemer G. Bcl-2 family members: dual regulators of apoptosis and autophagy. *Autophagy* 2008; **4**: 600–606.
13. Maiuri MC, Zalckvar E, Kimchi A, Kroemer G. Self-eating and self-killing: crosstalk between autophagy and apoptosis. *Nat Rev Mol Cell Biol* 2007; **8**: 741–752.
14. Pattingre S, Tassa A, Qu X, Garuti R, Liang XH, Mizushima N *et al.* Bcl-2 antiapoptotic proteins inhibit Beclin 1-dependent autophagy. *Cell* 2005; **122**: 927–939.
15. Maiuri MC, Le Toumelin G, Criollo A, Rain JC, Gautier F, Juin P *et al.* Functional and physical interaction between Bcl-X(L) and a BH3-like domain in Beclin-1. *EMBO J* 2007; **26**: 2527–2539.
16. Wei Y, Pattingre S, Sinha S, Bassik M, Levine B. JNK1-mediated phosphorylation of Bcl-2 regulates starvation-induced autophagy. *Mol Cell* 2008; **30**: 678–688.
17. Sarkar S, Floto RA, Berger Z, Imarisio S, Cordenier A, Pasco M *et al.* Lithium induces autophagy by inhibiting inositol monophosphatase. *J Cell Biol* 2005; **170**: 1101–1111.
18. Williams A, Sarkar S, Cuddon P, Ttofi EK, Saiki S, Siddiqi FH *et al.* Novel targets for Huntington's disease in an mTOR-independent autophagy pathway. *Nat Chem Biol* 2008; **4**: 295–305.
19. Gordon PB, Holen I, Fosse M, Rotnes JS, Seglen PO. Dependence of hepatocytic autophagy on intracellularly sequestered calcium. *J Biol Chem* 1993; **268**: 26107–26112.
20. Brady NR, Hamacher-Brady A, Yuan H, Gottlieb RA. The autophagic response to nutrient deprivation in the hl-1 cardiac myocyte is modulated by Bcl-2 and sarco/endoplasmic reticulum calcium stores. *FEBS J* 2007; **274**: 3184–3197.
21. Gao W, Ding WX, Stolz DB, Yin XM. Induction of macroautophagy by exogenously introduced calcium. *Autophagy* 2008; **4**: 754–761.
22. Hoyer-Hansen M, Bastholm L, Szyniarowski P, Campanella M, Szabadkai G, Farkas T *et al.* Control of macroautophagy by calcium, calmodulin-dependent kinase kinase-beta, and Bcl-2. *Mol Cell* 2007; **25**: 193–205.
23. Berridge MJ, Bootman MD, Roderick HL. Calcium signalling: dynamics, homeostasis and remodelling. *Nat Rev Mol Cell Biol* 2003; **4**: 517–529.
24. Szabadkai G, Bianchi K, Varnai P, De Stefani D, Wieckowski MR, Cavagna D *et al.* Chaperone-mediated coupling of endoplasmic reticulum and mitochondrial Ca2+ channels. *J Cell Biol* 2006; **175**: 901–911.
25. Szabadkai G, Rizzuto R. Participation of endoplasmic reticulum and mitochondrial calcium handling in apoptosis: more than just neighborhood? *FEBS Lett* 2004; **567**: 111–115.
26. Berridge MJ. The endoplasmic reticulum: a multifunctional signaling organelle. *Cell Calcium* 2002; **32**: 235–249.
27. Rong Y, Distelhorst CW. Bcl-2 protein family members: versatile regulators of calcium signaling in cell survival and apoptosis. *Annu Rev Physiol* 2008; **70**: 73–91.
28. Kroemer G, Galluzzi L, Brenner C. Mitochondrial membrane permeabilization in cell death. *Physiol Rev* 2007; **87**: 99–163.
29. Criollo A, Maiuri MC, Tasdemir E, Vitale I, Fiebig AA, Andrews D *et al.* Regulation of autophagy by the inositol trisphosphate receptor. *Cell Death Differ* 2007; **14**: 1029–1039.
30. Criollo A, Vicencio JM, Tasdemir E, Maiuri MC, Lavandero S, Kroemer G. The inositol trisphosphate receptor in the control of autophagy. *Autophagy* 2007; **3**: 350–353.
31. Lam D, Golstein P. A specific pathway inducing autophagic cell death is marked by an IP3R mutation. *Autophagy* 2008; **4**: 349–350.
32. Lam D, Kosta A, Luciani MF, Golstein P. The Inositol 1,4,5-Trisphosphate Receptor Is Required to Signal Autophagic Cell Death. *Mol Biol Cell* 2008; **19**: 691–700.
33. Klionsky DJ, Abeliovich H, Agostinis P, Agrawal DK, Aliev G, Askew DS *et al.* Guidelines for the use and interpretation of assays for monitoring autophagy in higher eukaryotes. *Autophagy* 2008; **4**: 151–175.
34. Mizushima N, Yoshimori T. How to interpret LC3 immunoblotting. *Autophagy* 2007; **3**: 542–545.
35. Mikoshiba K. IP3 receptor/Ca2+ channel: from discovery to new signaling concepts. *J Neurochem* 2007; **102**: 1426–1446.
36. Mikoshiba K. The IP3 receptor/Ca2+ channel and its cellular function. *Biochem Soc Symp* 2007; **74**: 9–22.
37. Varnai P, Balla A, Hunyady L, Balla T. Targeted expression of the inositol 1,4,5-triphosphate receptor (IP3R) ligand-binding domain releases Ca2+ via endogenous IP3R channels. *Proc Natl Acad Sci USA* 2005; **102**: 7859–7864.
38. Jaimovich E, Mattei C, Liberona JL, Cardenas C, Estrada M, Barbier J *et al.* Xestospongin B, a competitive inhibitor of IP3-mediated Ca2+ signalling in cultured rat myotubes, isolated myonuclei, and neuroblastoma (NG108-15) cells. *FEBS Lett* 2005; **579**: 2051–2057.
39. Gafni J, Munsch JA, Lam TH, Catlin MC, Costa LG, Molinski TF *et al.* Xestospongins: potent membrane permeable blockers of the inositol 1,4,5-trisphosphate receptor. *Neuron* 1997; **19**: 723–733.
40. Guillemette J, Caron AZ, Regimbald-Dumas Y, Arguin G, Mignery GA, Boulay G *et al.* Expression of a truncated form of inositol 1,4,5-trisphosphate receptor type III in the cytosol of DT40 triple inositol 1,4,5-trisphosphate receptor-knockout cells. *Cell Calcium* 2005; **37**: 97–104.
41. Devogelaere B, Verbert L, Parys JB, Missiaen L, De Smedt H. The complex regulatory function of the ligand-binding domain of the inositol 1,4,5-trisphosphate receptor. *Cell Calcium* 2008; **43**: 17–27.

42. Quirion JC, Sevenet T, Husson HP, Weniger B, Debitus C. Two new alkaloids from Xestospongia sp., a New Caledonian sponge. *J Nat Prod* 1992; **55**: 1505–1508.
43. Grynkiewicz G, Poenie M, Tsien RY. A new generation of Ca2+ indicators with greatly improved fluorescence properties. *J Biol Chem* 1985; **260**: 3440–3450.
44. Chiesa A, Rapizzi E, Tosello V, Pinton P, de Virgilio M, Fogarty KE *et al.* Recombinant aequorin and green fluorescent protein as valuable tools in the study of cell signalling. *Biochem J* 2001; **355**: 1–12.
45. Palmer AE, Jin C, Reed JC, Tsien RY. Bcl-2-mediated alterations in endoplasmic reticulum Ca2+ analyzed with an improved genetically encoded fluorescent sensor. *Proc Natl Acad Sci USA* 2004; **101**: 17404–17409.
46. Gonzalez-Polo RA, Boya P, Pauleau AL, Jalil A, Larochette N, Souquere S *et al.* The apoptosis/autophagy paradox: autophagic vacuolization before apoptotic death. *J Cell Sci* 2005; **118**: 3091–3102.
47. Criollo A, Galluzzi L, Maiuri MC, Tasdemir E, Lavandero S, Kroemer G. Mitochondrial control of cell death induced by hyperosmotic stress. *Apoptosis* 2007; **12**: 3–18.
48. Boya P, Gonzalez-Polo RA, Casares N, Perfettini JL, Dessen P, Larochette N *et al.* Inhibition of macroautophagy triggers apoptosis. *Mol Cell Biol* 2005; **25**: 1025–1040.
49. Jiang M, Milner J. Bcl-2 constitutively suppresses p53-dependent apoptosis in colorectal cancer cells. *Genes Dev* 2003; **17**: 832–837.
50. Harborth J, Elbashir SM, Bechert K, Tuschl T, Weber K. Identification of essential genes in cultured mammalian cells using small interfering RNAs. *J Cell Sci* 2001; **114**: 4557–4565.
51. Kabeya Y, Mizushima N, Ueno T, Yamamoto A, Kirisako T, Noda T *et al.* LC3, a mammalian homologue of yeast Apg8p, is localized in autophagosome membranes after processing. *EMBO J* 2000; **19**: 5720–5728.
52. Lin X, Varnai P, Csordas G, Balla A, Nagai T, Miyawaki A *et al.* Control of calcium signal propagation to the mitochondria by inositol 1,4,5-trisphosphate-binding proteins. *J Biol Chem* 2005; **280**: 12820–12832.

Supplementary Information accompanies the paper on Cell Death and Differentiation website (http://www.nature.com/cdd)